

## Techniques for Semi-Empirical Characterization of Material and Sensor Properties in Interdigital Dielectrometry

A. Mamishev and M. Zahn

Massachusetts Institute of Technology

Department of Electrical Engineering and Computer Science

Laboratory for Electromagnetic and Electronic Systems

Cambridge, MA 02139

**Abstract:** Interdigital frequency-wavenumber dielectrometry can be used for measurement of dielectric properties of insulating materials. It is not always possible to adequately model distributed circuit parameters of the sensor structure. Even in cases when the forward problem can be solved, that is, the distribution of electric field can be calculated using numerical techniques, it may not be suitable for the solution of the inverse problem due to the high sensitivity of the parameter estimation algorithms to variations in circuit and material parameters as well as non-ideality in the models due to finite size of the sensor, fringing field effects, and lead effects. This paper particularly shows the advantage of changing the function of the conducting plane beneath the interdigital electrode structure from a ground plane to a guard electrode that follows the sensing electrode voltage.

The techniques presented in this paper build a bridge between idealized models of interdigital structures and real measurements. Employment of such techniques allows experimental calibration of the sensor, verification of the intermediate steps in the process of development of parameter estimation algorithms, and provide data necessary for improvement of experimental arrangements.

### INTRODUCTION

Several theoretical studies for  $\omega$ - $k$  (frequency-wavenumber) dielectrometry technology have been conducted over the last decade [1]. Efforts have been made to utilize developed circuit models and electronic circuitry for various practical applications, mainly in the field of dielectric materials characterization [2]. The repeatability and precision of measurements based on this approach varies depending on a particular application. Recent experiments revealed noticeable differences between the theoretically predicted response of an interdigital sensor and measurements. The search and analysis of possible sources of such discrepancies as well as improved characterization methods are the subject of this paper.

Specifically, calculation and measurement of interelectrode capacitance and conductance is discussed. As is commonly done for capacitive sensors, the leads of the interdigital sensor are actively electrically guarded. As a result, it is not possible to measure values of interelectrode capacitance and conductance with a conventional two terminal connection. Alternatives to this approach are discussed.

A direct calibration of the sensor and reduction of the number of unknowns in the governing equation provides a dependable

way of determining the dielectric properties of a homogeneous material pressed against the sensor's working surface. The characterization of non-homogeneous materials requires a much more complex approach.

### DESCRIPTION OF THE SENSOR

The structure of the three-wavelength interdigital sensor used is shown in Figure 1. The sensor consists of three sets of electrodes deposited on a flexible polyimide substrate (Kapton). The sensing electrodes are shielded by guard electrodes driven by the buffer stage of the interface circuitry, and the guard electrodes are separated by ground electrodes. The sensor is connected to a microprocessor-controlled voltage source through electronic interface circuitry, which creates a resistive-capacitive divider, the output of which is recorded and analyzed.

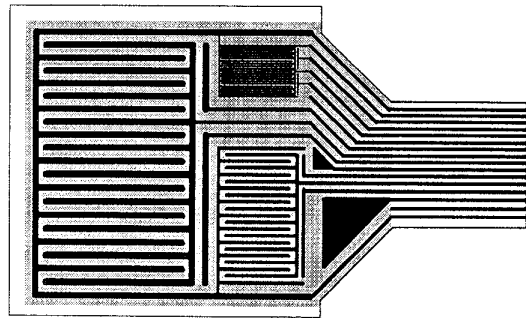


Figure 1. The three-wavelength interdigital sensor [2,3].

The cross-section of a half-wavelength of the sensor is shown in Figure 2. The parylene coating of 5  $\mu\text{m}$  thickness is necessary to prevent moisture absorption into the Kapton.

Using the lumped parameter representation of the sensor electrodes, the test response is equivalent to voltage gain and phase of an RC circuit shown in Figure 3. The sensor can potentially operate in two modes - with the ground plane being held at zero potential ( $V_T=0$ ), or guarded at the sensing electrode potential ( $V_T=V_S$ ). The voltage gain as a function of angular frequency  $\omega$  measured with  $V_T=0$  can be expressed as

$$G = \frac{V_S}{V_D} = \frac{G_{12} + j\omega C_{12}}{(G_{12} + j\omega C_{12})(1 + \alpha) + G_{11} + j\omega(C_{11} + C_L)}, \quad (1)$$

where

$$\alpha = \frac{2[G_{11} + j\omega(C_{11} + C_L)]}{j\omega C_P}, \quad (2)$$

$V_S$  is a measured voltage on a sensing electrode,  $V_D$  is the imposed voltage on a driven electrode, and  $C_P$  is the parylene coating capacitance on each electrode. When  $V_T = V_S$ , (1) and (2) are valid with  $G_{11}$  and  $C_{11}$  set to zero.

When operating in this guarded mode, the circuit can be solved directly for  $G_{12}$  and  $C_{12}$ , which can be mapped to permittivity  $\epsilon$  and conductivity  $\sigma$  of the test dielectric. In the case when the ground plane is held at zero potential, the equipotential lines are like those in Figure 4. In the case when the ground plane is held at the potential of a guard, there are no equipotential lines between the sensing electrode and the ground (now guard) plane.

When  $V_T$  is held at zero, the test dielectric material adjacent to the sensor primarily affects  $Y_{12} = G_{12} + j\omega C_{12}$ , while  $Y_{11} = G_{11} + j\omega C_{11}$  primarily depends on the dielectric properties of the Kapton substrate. However,  $Y_{11}$  is also affected by the unknown dielectric property of the test dielectric due to fringing field effects. A prime advantage of the guarded mode is that the complicating effects of  $Y_{11}$  are removed.

## DIRECT MEASUREMENTS

With the wavelength of the interdigital structure being on the order of millimeters, the capacitance  $C_{12}$  between the driven and sensing electrodes is around one pF, while the capacitance  $C_{11}$  between the sensing electrode and the ground plane is on the order of tens of pF. Often, the capacitance  $C_P$  of the parylene coating is so high compared with  $C_{12}$ , typically from 10 to 100 times  $C_{12}$ , that the parylene capacitance can be assumed to be a short circuit over most of the operating frequency range of .005 to 10,000 Hz ( $\alpha \approx 0$ ). Capacitance  $C_P$  can be estimated for each wavelength at very low frequency. Then (1) in the guarded mode reduces to  $G \approx 1/(1 + 2C_L/C_P)$ .

One advantage of the guarded mode can be easily seen if the material above the interelectrode structure is highly insulating, so that  $G_{11} \approx 0$  and  $G_{12} \approx 0$ . Then for the grounded mode the gain  $G$  in (1) is real, and with  $\alpha \approx 0$  it provides only one equation for two unknowns ( $C_{11}$  and  $C_{12}$ ). In the guarded mode with  $G_{11}$  and  $C_{11}$  effectively set to zero, (1) reduces to one equation in the unknown  $C_{12}$ . Similarly, if the test material is sufficiently conductive to have non-zero values of  $G_{11}$  and  $G_{12}$ , then the complex form of (1) in the grounded mode results in two equations in four unknowns ( $G_{11}$ ,  $C_{11}$ ,  $G_{12}$ , and  $C_{12}$ ). In the guarded mode, (1) reduces to two equations in two unknowns ( $G_{12}$  and  $C_{12}$ ).

For the grounded mode, one may try to add a resistor or a capacitor of known value to either branch in order to provide additional equations with the same unknowns. However, the precision of such an approach proved to be low because of the extremely high precision required in knowing element values.

Since the capacitance  $C_{11}$  is relatively high, it can also be measured using a conventional impedance meter in a standard three-terminal connection scheme where drive and sense electrodes are driven at the same potential with respect to the ground plane electrode.

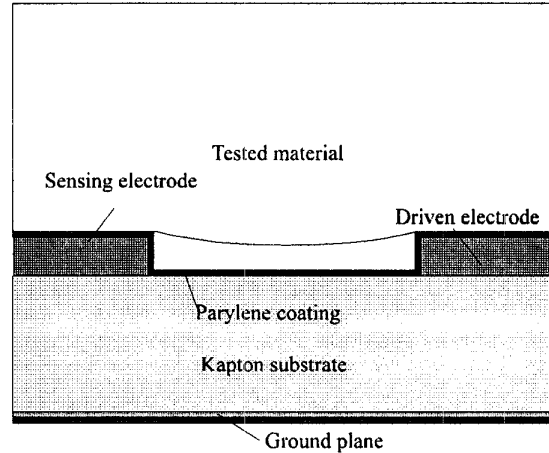


Figure 2. The cross-section of the interdigital sensor with a slightly flexible test material above it.

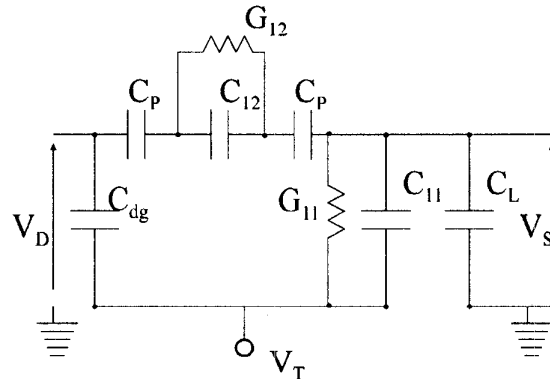


Figure 3. The equivalent circuit of each wavelength in the sensor of Figure 1.

Since the value of  $C_{12}$  is too low to accurately measure, it can be determined using (1) in the grounded mode after  $C_{11}$  has been found.

## COMPARISON OF CALCULATIONS AND MEASUREMENTS

The values of the interelectrode capacitances can also be found by modeling the structure of the interdigital sensor with finite element electric field software (FEM, Ansoft).

Distribution of equipotential field lines for the case when two layers of dielectric materials are placed above the sensor is shown in Figure 4. The distribution shown of the electric field

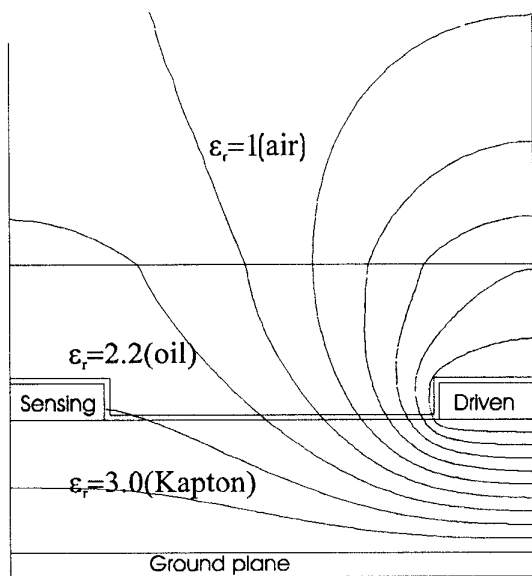


Figure 4. Equipotential field lines in the half-cell geometry of an interdigital sensor. Relative permittivity of parylene  $\epsilon_r=3.05$ . The driven electrode (right) is at 1 V potential, the sensing electrode (left) is at 0.2 V potential, and the ground plane is at 0 V.

is for the sensor working in the high frequency mode when conductance effects through the material are relatively unimportant.

A continuum model of an interdigital sensor [1] provides a closed-form solution for a set of idealized interdigitated electrodes (an infinite array of infinitely long microstrip conductors of zero thickness). A 2D finite-element model allows assumption of finite thickness of the electrodes as in Figure 4. Comparisons given in Table 1 demonstrates that although the continuum model of the interdigital sensor is theoretically adequate, the results of actual measurements may differ from predicted values by more than 30 percent. Several factors contribute to this, such as finite size of the interdigitated electrodes, non-zero metallization thickness of the electrodes, and, sometimes, poor contact between the materials on the sensor-tested material boundary.

**Table 1. Comparison of calculated and measured values of the interelectrode capacitances in air.**

(pF)	$\lambda=1.0$ mm		$\lambda=2.5$ mm		$\lambda=5.0$ mm	
	$C_{11}$	$C_{12}$	$C_{11}$	$C_{12}$	$C_{11}$	$C_{12}$
Continuum Model	11.8	1.19	24.6	0.54	89.1	0.80
FEM (Ansoft)	10.7	1.01	23.4	0.56	88.8	0.80
Direct Measurement	17.1	1.24	32.8	0.67	112	0.82

The measured values in Table 1 were obtained by combinations of guarded mode and grounded mode measurements together with capacitance meter measurements

of  $C_{11}$ . The values given in Table 1 were self-consistent between different measurement methods.

### EMPIRICAL CALIBRATION OF SENSOR

Calibration of  $C_{12}$  versus the permittivity of the test dielectric  $\epsilon$  is performed using materials with known permittivity verified by capacitive measurements with parallel plate electrodes.

Since  $\epsilon$  of air has a most reliable value ( $\epsilon_0$ ), the calibration is performed according to the formula:

$$C_{12} = C_0 + (\epsilon / \epsilon_0 - 1)S, \quad (3)$$

where  $C_0$  is the measured capacitance at  $\epsilon=\epsilon_0$ , and the slope  $S = dC_{12}/d(\epsilon/\epsilon_0)$  is the slope of the fitted line that goes through the origin. Consequently,  $\epsilon$  is found as:

$$\epsilon / \epsilon_0 = 1 + (C_{12} - C_0) / S. \quad (4)$$

An example of such a calibration is shown in Table 2. The values of  $C_0$  in Table 2 for air are slightly different from corresponding values in Table 1, because of small changes in configuration for guarding the previous ground plane.

**Table 2. High frequency calibration in the guarded mode of the three-wavelength sensor.**

Material	$\epsilon/\epsilon_0$	$\lambda=1.0$ mm $S \approx 0.61$		$\lambda=2.5$ mm $S \approx 0.53$		$\lambda=5.0$ mm $S \approx 0.77$	
		G, dB	$C_{12}$ , pF	G, dB	$C_{12}$ , pF	G, dB	$C_{12}$ , pF
Air ( $C_0$ )	1.0	-33.1	1.34	-29.6	0.80	-28.7	0.89
Teflon	2.1	-29.7	2.02	-24.9	1.41	-23.2	1.74
Polyethylene	2.3	-28.9	2.22	-24.4	1.49	-22.7	1.85
Lexan	3.2	-27.5	2.62	-22.4	1.92	-20.0	2.58
Delrin	3.6	-26.3	2.93	-18.4	2.18	-19.4	2.83

Results of experiments with oil-free transformer pressboard in air are shown in Figure 5. The shape of the phase curve in Figure 5 differs from an ideal one-pole system primarily due to the dependence of the complex permittivity of the dispersive pressboard on the frequency of applied electric field. Estimation of the numerical values of  $C_p$  and evaluation of its importance can be done based on the leftmost part of the gain curve in Figure 5. At the lowest frequency all three wavelengths have approximately zero phase, so that the gain is real in agreement with (1) in the guarded mode at very low frequency. From the gain value at low frequency the value of  $C_p$  for the 1, 2.5, and 5 mm wavelengths are calculated to be about 10, 20, and 80 pF, with  $C_L$  respectively 60, 24, and 23 pF. The  $C_p$  values are in the appropriate ratio to electrode areas as expected and are due to parylene capacitance in series with a small air gap due to the surface texture of pressboard. Solution of the inverse problem for a complex dielectric permittivity ( $\epsilon=\epsilon'-j\epsilon''$ ) for this material are shown in Figures 6 and 7. The permittivity measurements ( $\epsilon'$ ) are most accurate at high frequencies while the conductivity ( $\epsilon''=\sigma/\omega$ ) is most accurate in the mid-frequency range. For a homogenous material, all three wavelengths should indicate approximately equal values of  $\epsilon'$  and  $\epsilon''$  while  $G_{12}$  and  $C_{12}$  will

be different for each wavelength as the electrode lengths and spacings are different.

However, the calibration of  $\epsilon''$  versus  $G_{12}$  has been done with pressboard in a parallel plate sensor, similarly to the Table 2 capacitive measurements. However, the results are not very reliable, partially due to low repeatability of the measurement. Only smooth, rigid, slightly compressible materials can be used for precise calibration for  $\sigma$ , whereas pressboard has a surface texture pattern. In general, intimacy of contact, and, consequently, applied pressure, plays an important role and may potentially introduce very large errors in the parameter estimation process. In addition, slight surface contamination of the sensor itself may affect calibration of highly insulating materials.

The slope of  $\epsilon''$  is not strongly affected by calibration. In our case, it is equal to  $\approx -0.6$ , obtained both with the three-wavelength sensor as well as with parallel plate capacitor measurements.

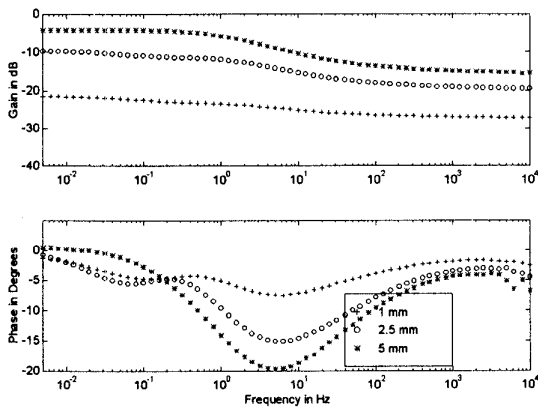


Figure 5. Gain and phase for the three-wavelength sensor with guarded sensing electrode, with a thick layer (4mm) of oil-free transformer pressboard pressed against the surface of the sensor.

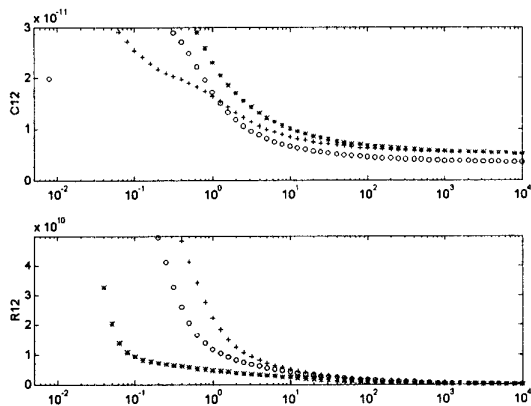


Figure 6. Pressboard in air - solution of the inverse problem for a homogeneous material. The values of  $R_{12}=1/G_{12}$  and  $C_{12}$  are obtained from gain/phase measurements of Figure 5.

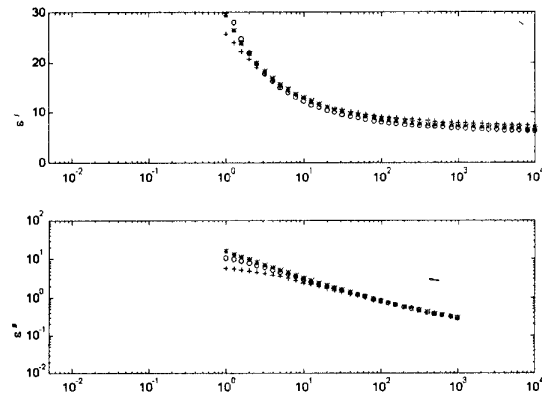


Figure 7. Pressboard in air - values of  $\epsilon'$  and  $\epsilon''$  obtained from Figure 6 using the calibration data of Table 2.

## CONCLUSIONS

Application of  $\omega-k$  interdigital dielectrometry for characterization of insulation materials requires refinement and verification of idealized theoretical models.

Feasibility of the direct calibration approach for the purposes of homogeneous material characterization, and, more importantly, verification of more complete algorithms for parameter estimation, is demonstrated. Comparison between theoretical predictions and actual measurements is made. An example inverse problem of parameter estimation is solved for transformer pressboard. The advantages of guarded mode measurements are demonstrated.

## ACKNOWLEDGMENTS

The authors would like to acknowledge the support of the Electric Power Research Institute, under grant WO 3334-1, managed by Mr. S. Lindgren, and the National Science Foundation under grant No. ECS-9523128. The donation of Maxwell software by Ansoft Corp. is gratefully appreciated. The authors would like to thank Mr. Darrell Schlicker, Ms. Yanqing Du, and Prof. B. Lesieutre, all from the MIT Laboratory for Electromagnetic and Electronic Systems, for valuable discussions and assistance with the experiments.

## REFERENCES

1. Zaretsky, M.C., L. Mouayad, and J.R. Melcher, "Continuum Properties from Interdigital Electrode Dielectrometry," IEEE Transactions on Electrical Insulation, Vol. 23, No.6, December 1988, pp. 897-917.
2. von Guggenberg, P.A., and J.R. Melcher, "A Three-wavelength Flexible Sensor for Monitoring the Moisture Content of Transformer Pressboard", Proc. of the 3rd International Conference on Properties and Applications of Dielectric Materials, Vol. 2, pp. 1262-5.
3. Marnishev, A.V., Y. Du, and M. Zahn, "Measurement of Dielectric Property Distributions Using Interdigital Dielectrometry Sensors," IEEE Conference on Electrical Insulation and Dielectric Phenomena, Virginia Beach, VA, October 1995, pp. 309-311.